VALIDATION AND DEVELOPMENT OF THE HIGH-RESOLUTION SEMI-LAGRANGIAN ECMWF FORECAST MODEL

A J Simmons
European Centre for Medium-Range Weather Forecasts
Reading, UK

Abstract

An account is given of the development of the T213/L31 ECMWF forecast model over the year since its operational implementation. This supplements the reports on this new model presented at the 1991 Seminar. Some of the problems experienced in the initial operational use of the model are summarized. Specific consideration is given to the formulation of the semi-Lagrangian scheme, in particular to the use of a "vertically non-interpolating" version. Some of the biases in low-level temperature are also discussed. Results are presented from the pre-operational validation of an improved version of the model which was introduced operationally in mid-August.

1. INTRODUCTION

A major change to the operational ECMWF forecast model was made on 17 September 1991. Horizontal resolution was doubled, and vertical resolution was similarly increased over much of the troposphere and lower stratosphere. Besides the increase in resolution of the new T213/L31 model, the following changes were made:

(i) use of a reduced Gaussian grid for the computations carried out in physical space. The number of grid points along a latitude circle now decreases towards the poles, to make the spacing of points approximately 60km over the whole globe at T213 resolution.

(ii) use of a semi-Lagrangian advection scheme. Changes in time step, time filter and horizontal diffusion were made in conjunction with the change in resolution and numerical scheme.

(iii) use of modified physical parametrizations. The principal change was in the treatment of clouds and radiation, to give better performance at the new 31-level vertical resolution. Some changes were also made to the vertical diffusion and convection routines with the aim of ensuring either more accurate or more stable integrations using the longer time steps made possible by the semi-Lagrangian method.

With such a radical change in resolution and numerical scheme, it is perhaps not surprising that a number of problems were encountered with the new model version in its developmental phase and in subsequent operational use. Considerable effort has been devoted to these problems over the past year, and a number of changes have been introduced operationally.

The aim of the lecture given at this Seminar was twofold. The first was to illustrate the principal types of validation used in the pre- and post-operational development of the new model. The second was to present some of the benefits of increased resolution, the working of the semi-Lagrangian scheme, and the steps taken to tackle some of the problems encountered. A substantial part of the material shown had in fact been presented also at the preceding ECMWF Seminar on Numerical Methods in Atmospheric Models

(*Hortal*, 1991; *Simmons*, 1991), and will not be repeated in this written account. Instead, we concentrate here on the work carried out to improve the model in the year since its operational implementation.

The first phase of this work was the assessment of the early operational performance of the model and investigation of comments received on the quality of the forecasts. Here it was necessary to distinguish problems that were genuinely due to the change in resolution or numerical scheme from problems that were associated with long-standing model deficiencies or short-term data problems. In particular, very poor performance in the Southern Hemisphere in November and early December was found to be caused primarily by problems with satellite data rather than (as initially suspected) a new model problem. These investigations were helped by a collaboration with DWD, which was undertaken to enable the ECMWF model to be run from initial analyses produced by DWD's operational T106/L19 system.

Several specific errors or deficiencies were corrected during the period from November 1991 to June 1992. These are discussed in the following section. Particular aspects of the numerical formulation (section 3) and physical parametrizations (section 4) were also investigated, leading to a more substantial model change in August (section 5). Ongoing work is summarized in section 6.

2. EARLY PROBLEMS

Three errors in the model code were identified and corrected between November and May. Two were in the parametrization of radiation. The first was among a set of technical changes made to speed up the model just before operational implementation. An insufficiently discriminating look-up table was introduced, which had the effect of eliminating important absorbers in the upper troposphere and stratosphere. The problem was identified partly by synoptic diagnosis of isentropic potential vorticity (PV) maps (as discussed by Davies in these proceedings), which showed systematic drifts in values of PV in the lower stratosphere. It was also shown by routine monthly inspection of zonal-mean errors, which showed very much larger erroneous trends in upper tropospheric temperatures than seen previously. Pre-existing problems of excessive upper-tropospheric radiative cooling and excessive eddy kinetic energy were made worse by the error, and this is likely to have been one (though certainly not the only) factor contributing to the increased day-to-day inconsistency of forecasts noted with the introduction of the new model. The error was corrected late in November.

The second problem was much more local in nature. A compiler error in the packing of radiative fields caused erroneous tendencies at a few isolated points of the reduced grid. It was revealed by routine monitoring of monthly-averaged radiation fields. A change in packing method was introduced in May to avoid this problem.

The third error was more dramatic in its occasional impact, and more difficult to track down. In the new model, a limiter was introduced for the parametrized convective mass fluxes to prevent computational instability when the large time steps made possible by the semi-Lagrangian advection scheme were used. The limiter was in fact incorrectly applied in the case of mid-level convection, making the scheme more unstable, rather than stable, at the few points where it was invoked. In practice this caused the model to fail three times in operations between December and March. In each case the operational forecast was completed either by reducing the time step from 20 to 15 min or by increasing the horizontal diffusion. The error was finally traced and corrected in May.

It was decided to keep the model time step at 15 min following the model change in May. Also, a generally less scale-selective form of horizontal diffusion (introduced in mid-January) that gave more damping than adopted originally for wavenumbers smaller than 150 was retained. These choices were made partly for reasons of safety, and partly to reduce some noise problems that had been observed when using the 20 min time step. Further optimization of the code compensated for the computational cost of using the smaller time step.

Another reason for using the smaller time step was its contribution to the reduction of excessive convective precipitation in short- and early medium-range forecasts in the Tropics and summertime middle latitudes. In pre-operational trials this problem was seen to be substantially worse with the new high-resolution model than with the then-operational T106/L19 model, and when implementing the new model in September 1991 it was recognized that it was important to find a solution to this problem before the following summer. The smaller time step was a part of the solution that was indeed found, but the principal improvement came from the exclusion from the analysis of SYNOP-based humidity data over land, which was implemented operationally in June.

An illustration of the improved hydrological balance of the short-range forecasts is given in Fig. 1. The upper two panels show global-mean precipitation and evaporation rates as functions of forecast range for operational T106/L19 forecasts from 15 July 1990 and 1991. In both cases there is an initial imbalance in the budget, with relatively large values of precipitation and low values of evaporation. The lower panels show results for T213/L31 forecasts from the parallel run for 15 July 1991 and from operations for 15 July 1992. The substantially larger short-range precipitation of the new model for 15 July 1991 is evident. Also clear is the large improvement for the 1992 case. Monthly means for July 1992 in fact show that on average the net precipitation tends to increase over the first few forecast days. There remains an overprediction of precipitation in the short range over land, but this is more than compensated by an underprediction of short-range precipitation over sea.

3. SEMI-LAGRANGIAN FORMULATION

Tests carried out during the year showed that the performance of the standard operational version of the semi-Lagrangian scheme was somewhat poorer than that of the Eulerian scheme at T106/L31 resolution, particularly away from the ground and as measured by RMS errors. Levels of eddy kinetic energy were typically higher with this version of the semi-Lagrangian scheme, and this was thought to contribute to the increased inconsistency of the high resolution forecasts. The high values of eddy kinetic energy were particularly evident in tests of the semi-Lagrangian scheme at T63 resolution in extended integrations to establish the model climatology.

Several sensitivity studies were undertaken. Attention became concentrated on an alternative version of the semi-Lagrangian code which adopts the "non-interpolating" scheme of *Ritchie* (1991) for the vertical advection. This scheme, which is used operationally in Canada, was included originally as an option in the Centre's semi-Lagrangian code, but was not fully validated during the pre-operational development of this code. Tests of this option at T106/L31, and subsequently T213/L31, resolution have revealed a positive impact on objective measures of skill, as illustrated in Fig. 2. Moreover, levels of eddy activity are generally lower than with the fully interpolating scheme. Two synoptic examples are shown in Fig. 3. The predominant occurrence of positive forecast height differences near the bases of troughs and cut-off lows indicates that the vertically non-interpolating scheme reduces the tendency of the model to produce troughs

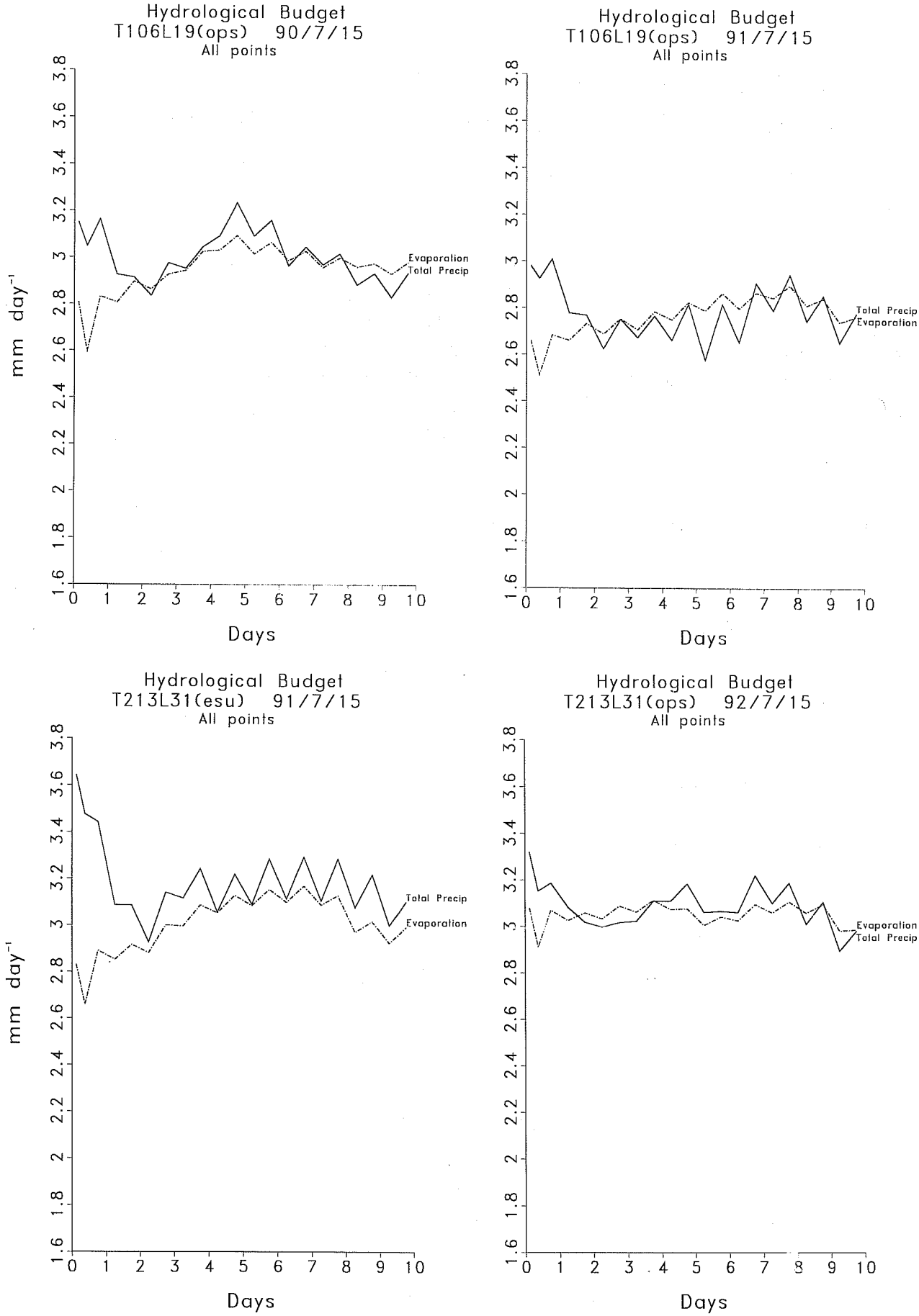

Fig. 1 Global-mean hydrological budgets for operational forecasts from 15 July for 1990, 1991 and 1992. Also shown (lower left) is the result for 15 July 1991 from the pre-operational trial of the T213/L31 model.

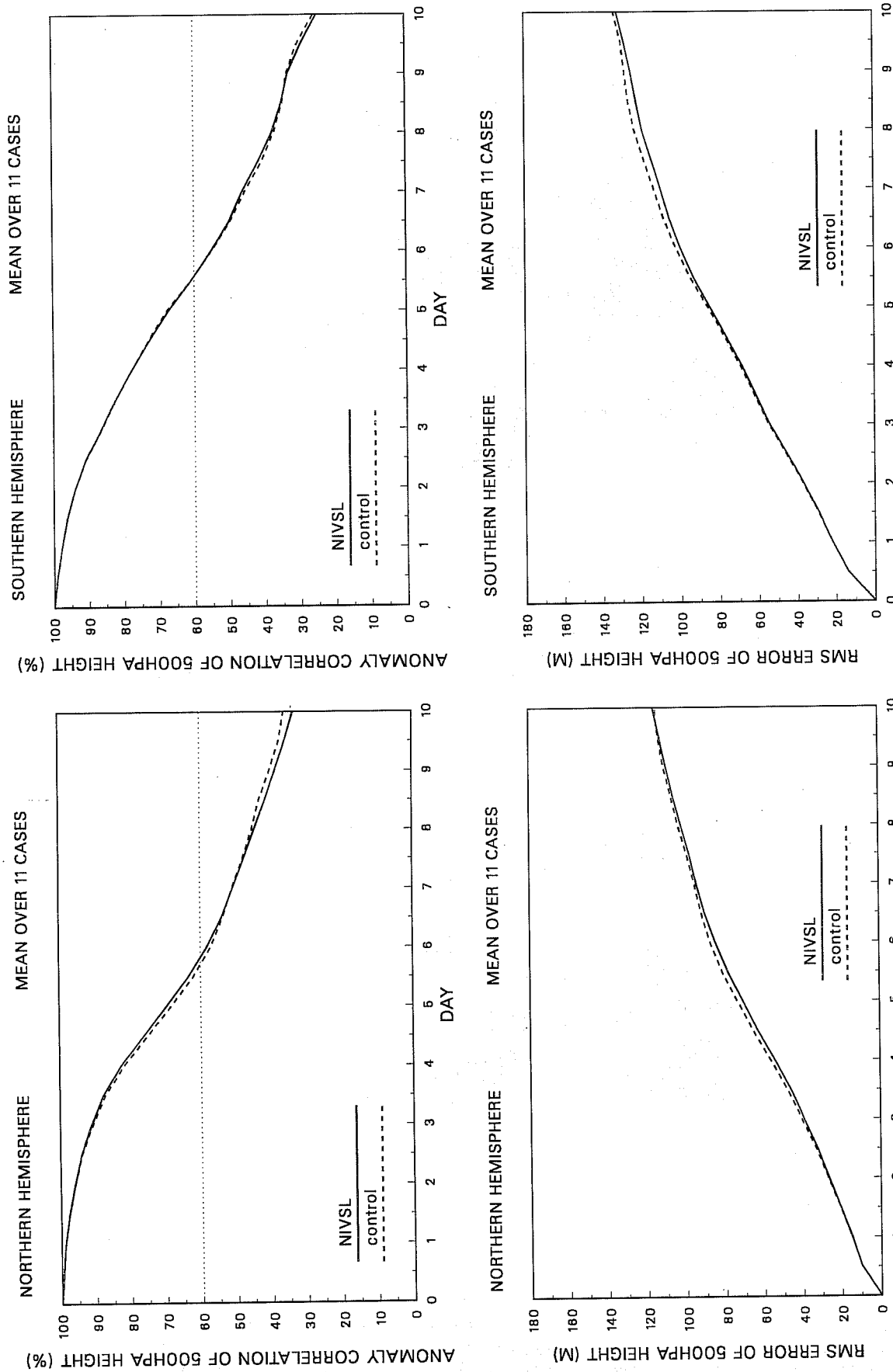

Fig. 2 500hPa height anomaly correlations and RMS errors for the extratropical Northern and Southern Hemispheres, using the "non-interpolating" vertical advection scheme (solid lines) and the standard fully interpolating semi-Lagrangian scheme (dashed lines). Averages over eleven cases (six using T106/L31 resolution and five using T213/L31) are shown.

Sunday 15 December 1991 12z ECMWF Forecast t+120 VT: Friday 20 December 1991 12z
500hPa height difference NIVSL-SL; SL

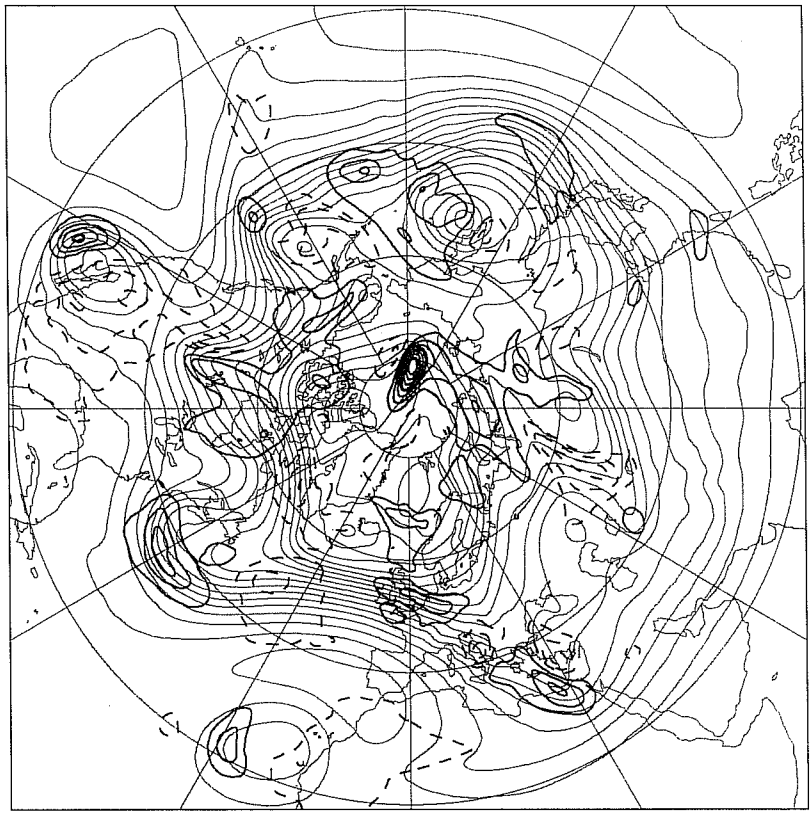

Wednesday 15 January 1992 12z ECMWF Forecast t+120 VT: Monday 20 January 1992 12z
500hPa height difference NIVSL-SL; SL

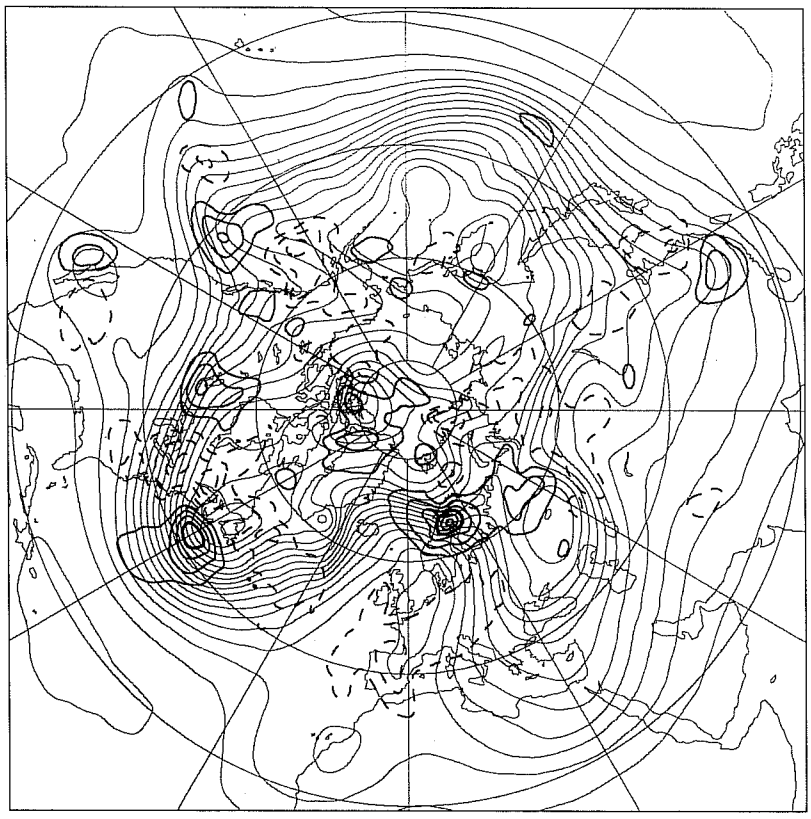

Fig. 3 Day-5 500hPa T213/L31 height forecasts from 15 December 1991 and 15 January 1992. The fine solid lines (contour interval 6dam) show the forecast made using the fully interpolating scheme. The heavier lines (contour interval 2dam, negative contours dashed) show differences between the "non-interpolating" and fully interpolating forecasts.

and cut-offs that are too intense and extend too far to the south. Corresponding plots of eddy kinetic energy are presented in Fig. 4. Lower eddy kinetic energies are found almost systematically when the non-interpolating scheme is used. Also, differences in zonal-mean temperature between semi-Lagrangian and Eulerian forecasts are substantially reduced at upper levels when the semi-Lagrangian scheme is changed to the non-interpolating form. Fig. 5 provides two examples.

A very slight further improvement in forecast skill has been achieved by reducing the strength of the time filter used in the semi-Lagrangian version to that used in the Eulerian version. Objective scores are presented in Fig. 6. The larger value of filter was originally needed to maintain computational stability of the convective parametrization when using relatively long time steps; this necessity disappeared when the calculation of the mass-flux limiter was corrected.

4. LOW-LEVEL COOLING

Large low-level temperature errors were noted in several places during late winter and spring. In March and April they were particularly pronounced over snow-covered regions of North America, and also over northern Europe and Siberia. Later in the season substantial errors occurred in the neighbourhood of the Baltic and North Sea. An example is presented in Fig. 7. Similar problems had been found in previous years, but errors were more marked with the new model.

Deficiencies in two aspects of the physical parametrization were principally responsible. Firstly, the model predicted stratiform boundary-layer clouds in the areas where the temperature errors were largest, whereas observations often showed clear skies. The parametrization concerned was the "inversion-cloud" scheme, the purpose of which is to simulate stratocumulus clouds based on the strength of the inversion and a relative humidity criterion. Such cloud was already prevented from forming in the lowest model layer, but occurred excessively in the next two layers over snow-covered land and relatively cold seas. Radiative cooling provided a positive feedback. As a quick remedy, the simple expedient of suppressing inversion cloud at these two levels was investigated. This gave some of the required warming, without serious loss of the stratocumulus that the scheme was intended to represent. The upper panel of Fig. 8 illustrates the impact on two-metre temperature in a two-day forecast from late May. Warming is seen over northern Europe, and also over part of the Mediterranean, where excessive low cloud has long been a problem in summer.

The second factor contributing to the low-level cooling was the treatment of the surface and boundary-layer fluxes. Three model problems that have impact on the surface temperature forecast were identified from a comparison with FIFE data (see Beljaars and Betts' contribution to these proceedings):

(i) lack of entrainment,
(ii) too slow response of surface temperature,
(iii) too much evaporation from wet surfaces, and too little in dry conditions.

The new parametrization discussed by Beljaars and Betts, including revised stability functions, skin effect, entrainment and increased stomal resistance, gives a warmer and drier boundary layer. The lower panel of Fig. 8 shows its impact on two-metre temperature for the May case already used to illustrate the effect of reduced inversion cloud. Warming is pronounced over land areas surrounding the Baltic and North Sea.

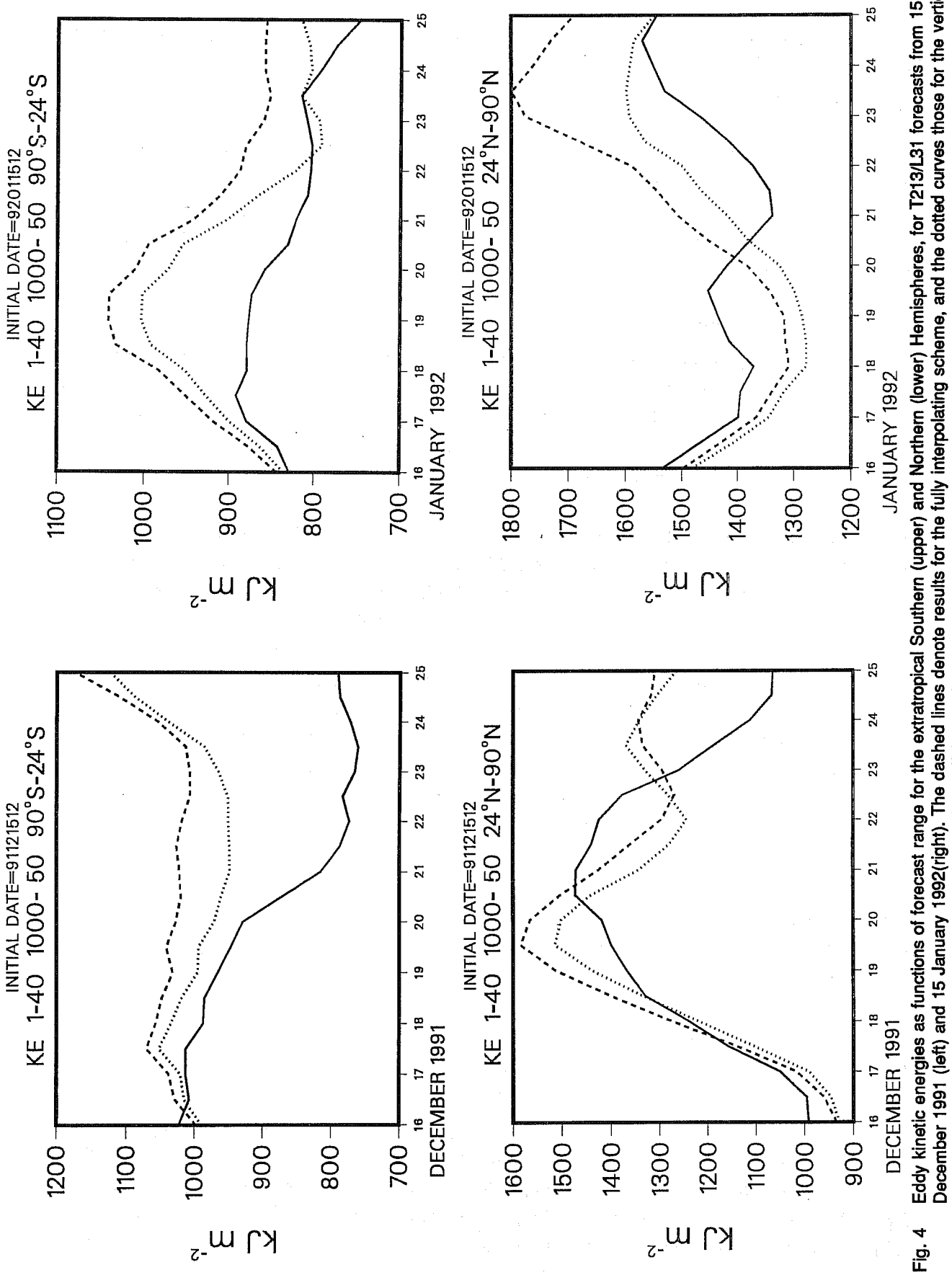

Fig. 4 Eddy kinetic energies as functions of forecast range for the extratropical Southern (upper) and Northern (lower) Hemispheres, for T213/L31 forecasts from 15 December 1991 (left) and 15 January 1992(right). The dashed lines denote results for the fully interpolating scheme, and the dotted curves those for the vertically non-interpolating scheme. The solid lines denote the verifying analyses.

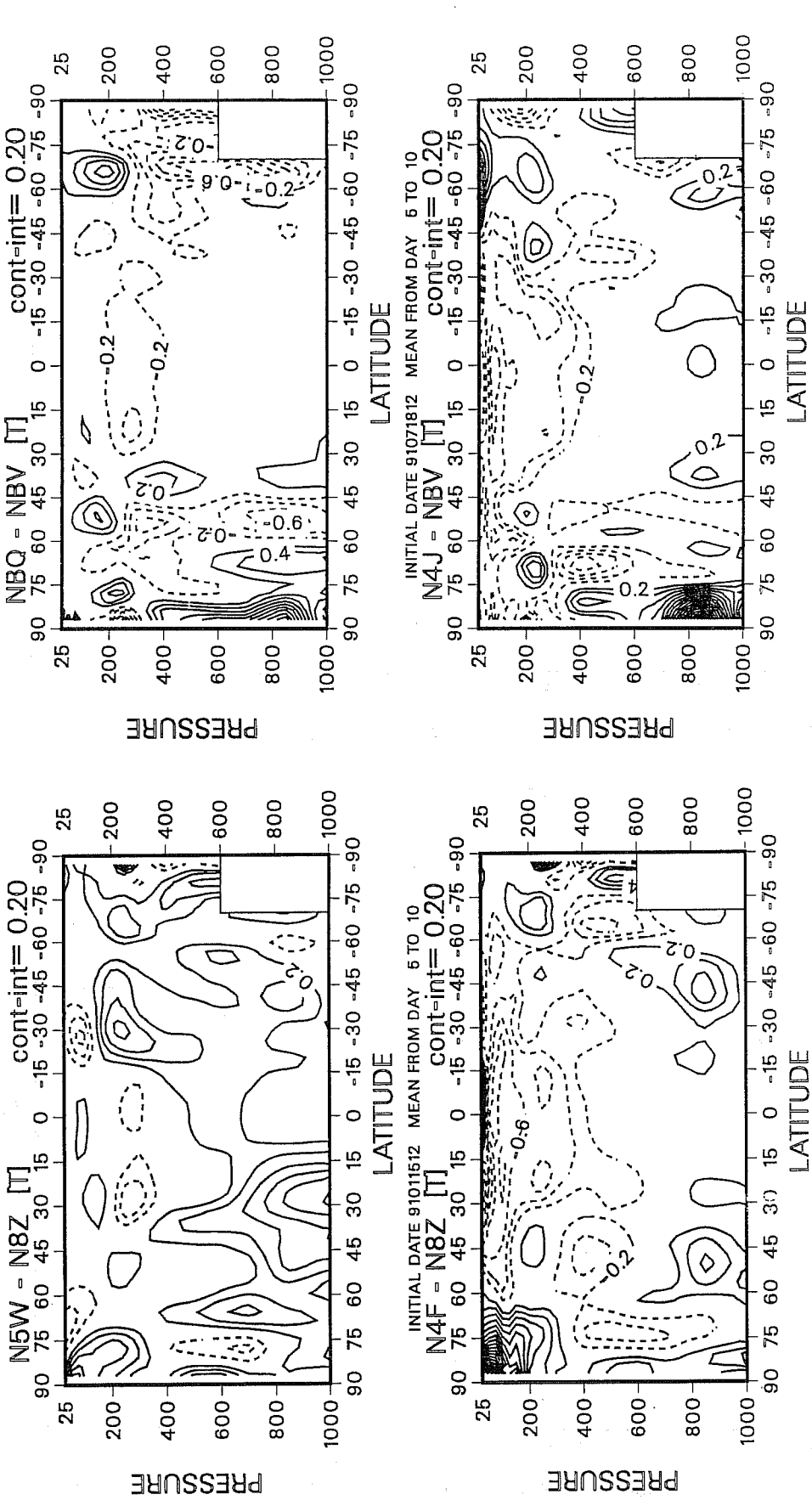

Fig. 5 Differences in zonal-mean temperature (K) averaged over forecast days 5-10 between Eulerian and vertically non-interpolating semi-Lagrangian forecasts (upper) and between Eulerian and fully interpolating semi-Lagrangian forecasts (lower), for T106/L31 forecasts from 15 January (left) and 18 July (right) 1991.

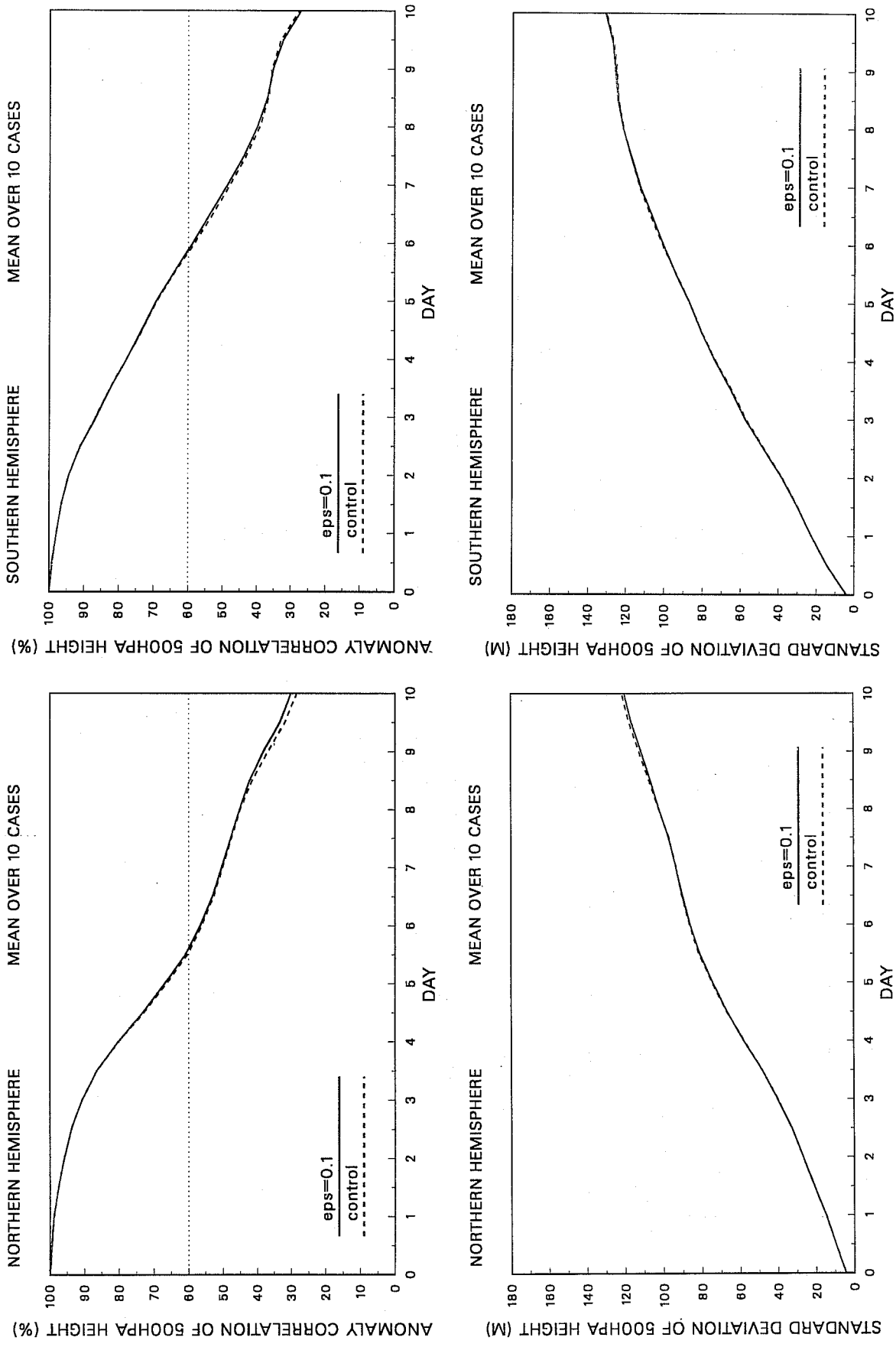

Fig. 6 500hPa height anomaly correlations and RMS errors for the extratropical Northern and Southern Hemispheres, using a time-filtering coefficient of 0.1 (solid lines) and 0.2 (dashed lines), averaged over ten T106/L31 forecasts.

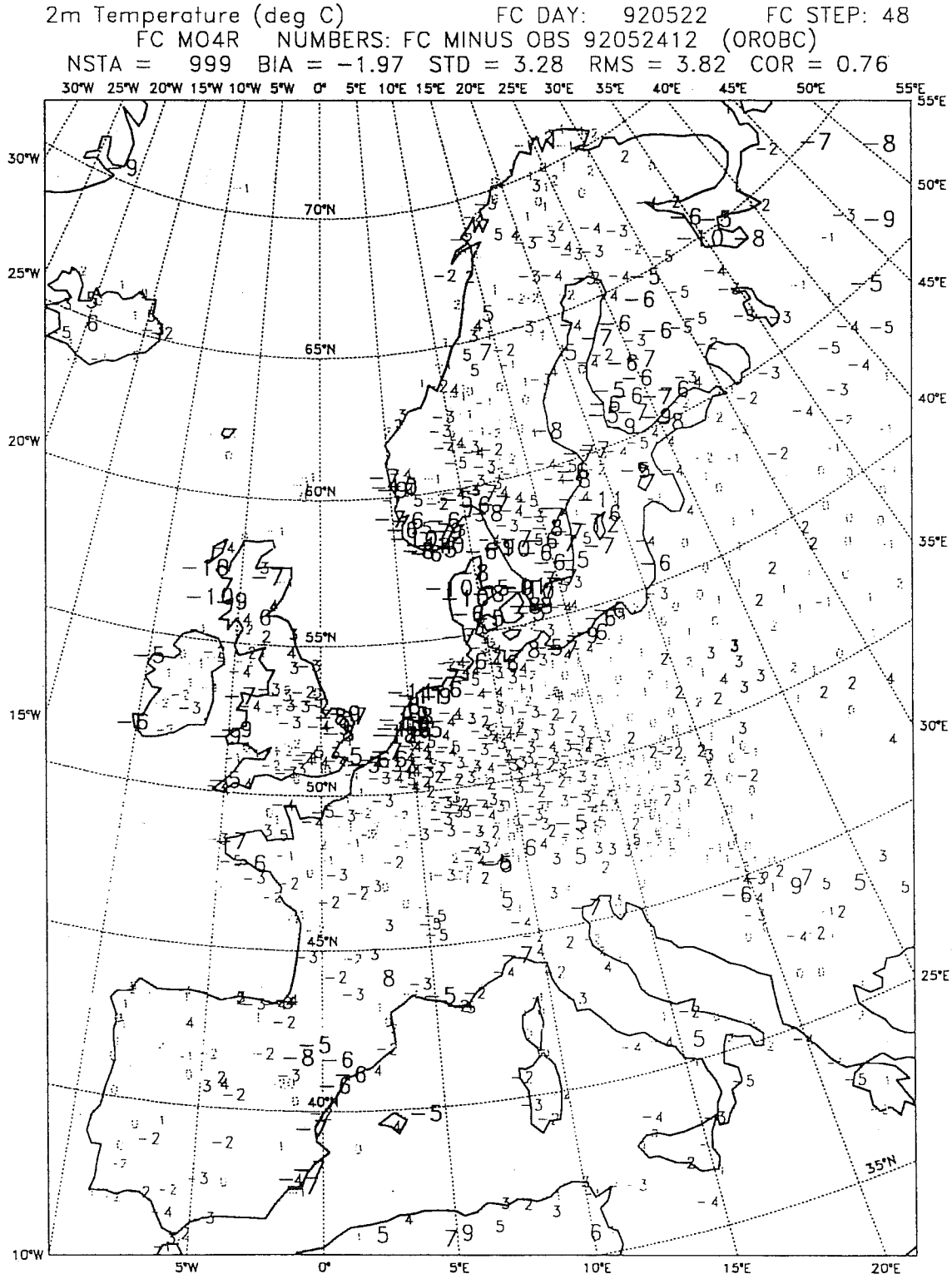

Fig. 7 Temperature errors at SYNOP stations for a 48-hour T106/L31 control forecast from 22 May 1992. These are very similar to the errors of the corresponding operational T213/L31 forecast.

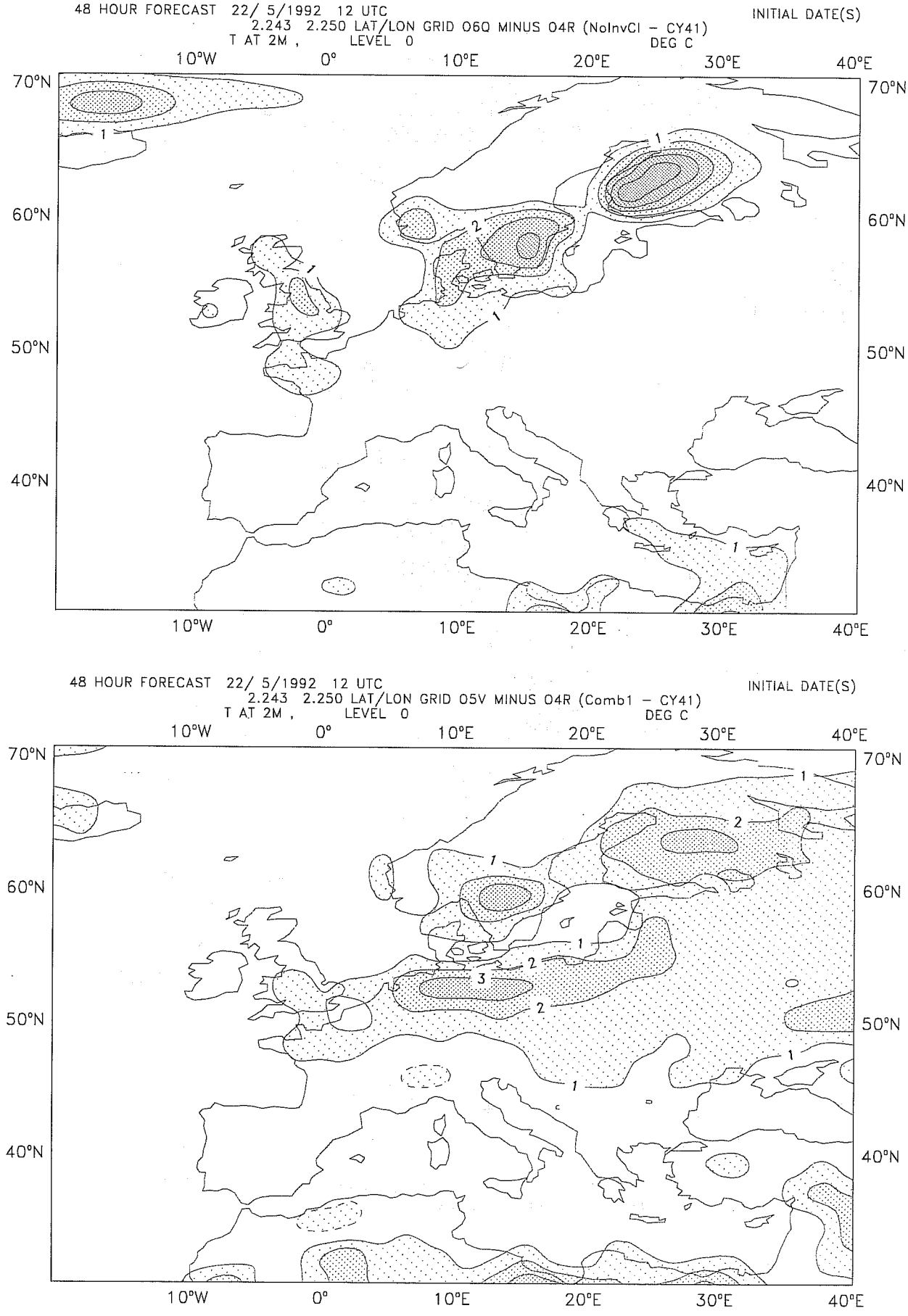

Fig. 8 Differences in 48-hour forecasts of two-metre temperature, showing the effects of suppressing low-level "inversion" cloud (upper map), and of the changes in treatment of boundary-layer and surface fluxes (lower map).

Fig. 9 shows the equivalent plot to Fig. 7 when the model is modified both to remove the low-level inversion cloud and to use the new surface and boundary-layer treatment. Strong cooling is here confined almost entirely to near-coastal stations. Warming over continental areas has, however, increased. It is believed to be due to an overestimation of solar radiation at the surface, due both to a general underestimation of daytime continental cloud and to a deficiency in the clear-sky radiation calculation. This is one reason why it was decided to choose only the removal of low-level inversion cloud for early operational implementation.

5. TESTS OF A NEW MODEL CYCLE

Based on the above results, a provisional new version of the operational model, cycle 43, was prepared. It included use of the vertically non-interpolating semi-Lagrangian scheme and smaller time filter, and suppression of the inversion cloud at the two extra model levels. Other modifications of a relatively minor nature were made to the cloud scheme. A simple slab representation of sea ice was introduced, giving a prognostic equation for ice-temperatures to replace the use of climatological values. Changes were made to remedy the failure of the radiation scheme to damp any vertical two-grid temperature waves, and to reduce the amount of cumulus momentum transfer.

This new model version was tested at T213/L31 resolution on a set of 12 cases drawn one from each month of the past year. For these experiments there was no data assimilation; the initial analyses were either from operations or from the pre-operational parallel runs of the high-resolution model. Mean anomaly correlations and RMS errors of the 500 hPa height field are presented in Fig. 10 for the extratropical hemispheres. The improvement brought about by use of cycle 43 is clear. Results are similar for other verification scores and most smaller domains. A selection for Europe is presented in Fig. 11.

A seven-day data assimilation experiment was performed for the period 13-19 January 1992. Assimilations were carried out using the operational system as of 1 July, and repeated using the new version of the model. The results enabled us to measure not only the impact of the proposed model change, but also the impact of the various operational changes made between January and July, the principal of which was the introduction of a one-dimensional variational method for processing satellite data (*Eyre et al.*, 1992).

500 hPa height scores for the extratropical Northern Hemisphere, and for Europe alone, are shown in Fig. 12. A clear improvement is seen to result both from the use of the July operational system and from the use of cycle 43. The latter appears to be particularly beneficial over Europe. It is probably optimistic to expect such a degree of improvement to hold over a period very much longer than the seven days examined here, but these results are nevertheless encouraging. The improvement can be clearly seen in synoptic maps. Fig. 13 provides examples based on three successive day-6 forecasts. A consistently better treatment by cycle 43 is seen for the high pressure over northern Europe, the cut-off over southwestern Europe, and the trough over eastern Europe.

A higher horizontal diffusion was used operationally between 15 January and 23 March because of the problems of computational stability noted previously. The cycle 43 forecasts also have lower damping due to the use of the smaller time filter. One effect is a significant *reduction* in noise seen in the tropospheric vertical velocity field in the vicinity of what can be quite modest orography. Fig. 14 provides an example. The noise shows also in corresponding patterns of precipitation. Its cause has yet to be determined, but its amelioration by the changes in model formulation made since last winter is clear. In addition to the effect

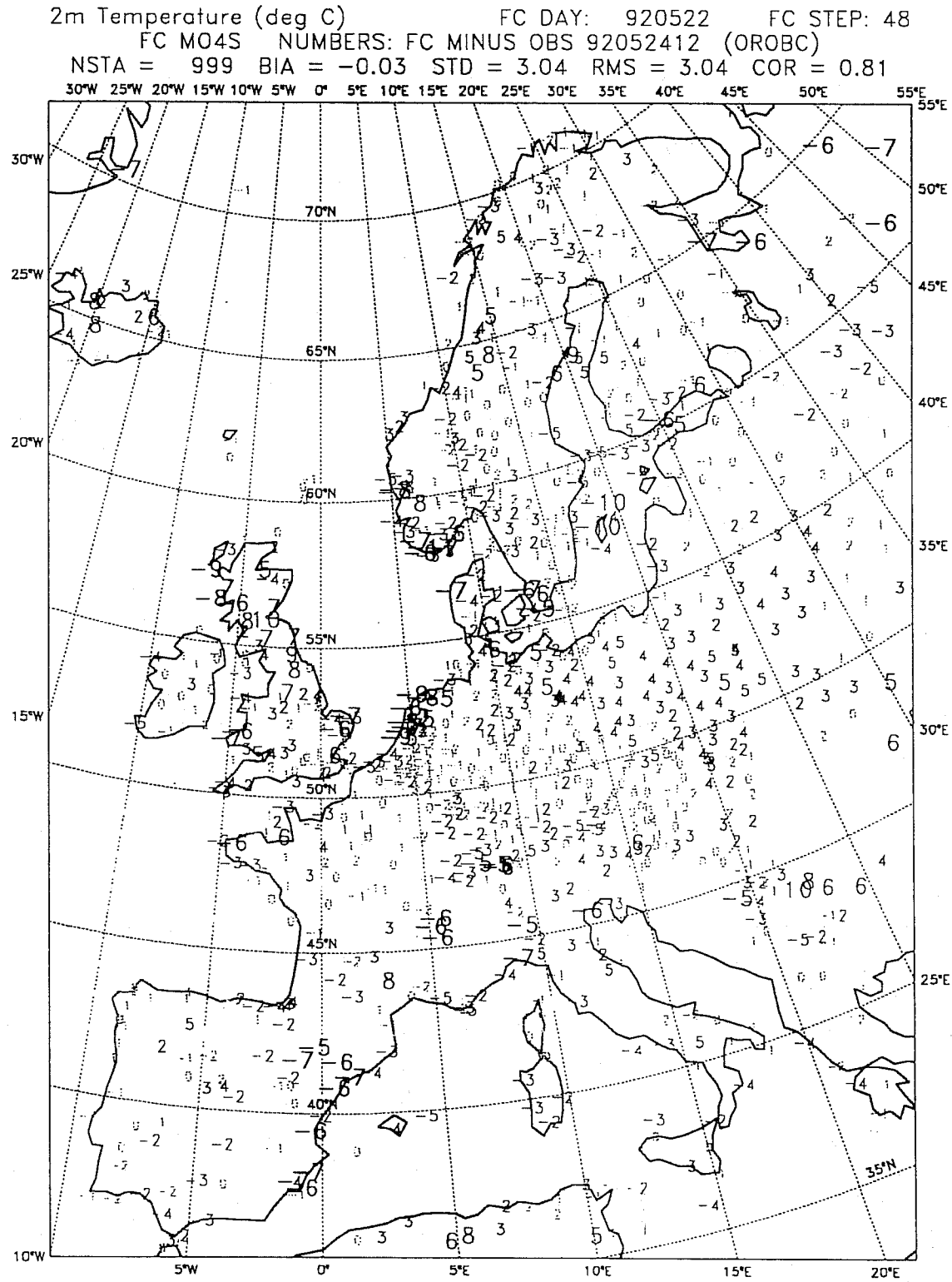

Fig. 9 Temperature errors at SYNOP stations as in Fig. 7 , but for forecasts with the new PBL scheme and no "inversion" cloud in the lowest three model levels.

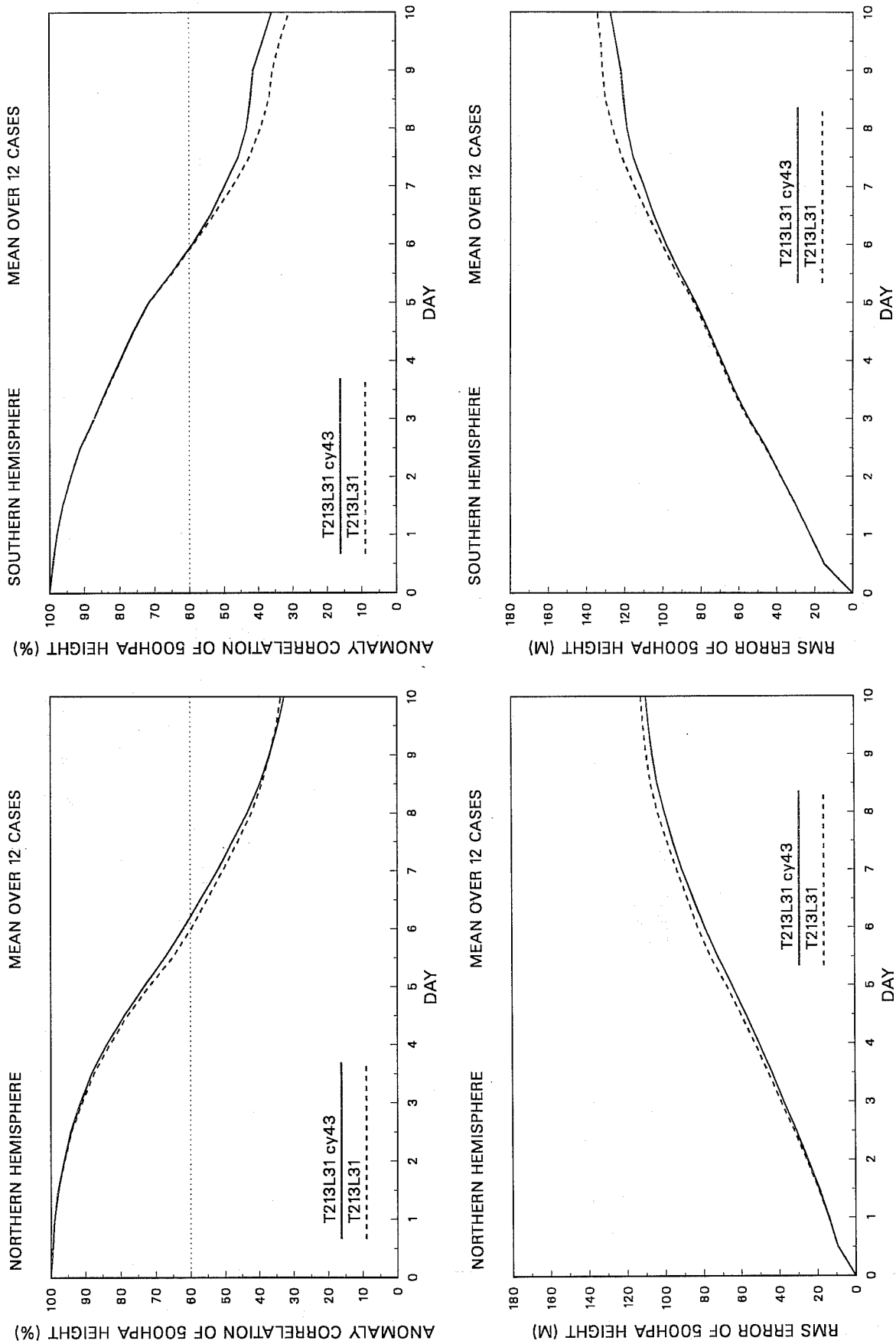

Fig. 10 500hPa height anomaly correlations and RMS errors for the extratropical Northern and Southern Hemispheres, using the initial version of model cycle 43 (solid lines) and model cycle 42 (dashed lines), averaged over twelve T213/L31 forecasts.

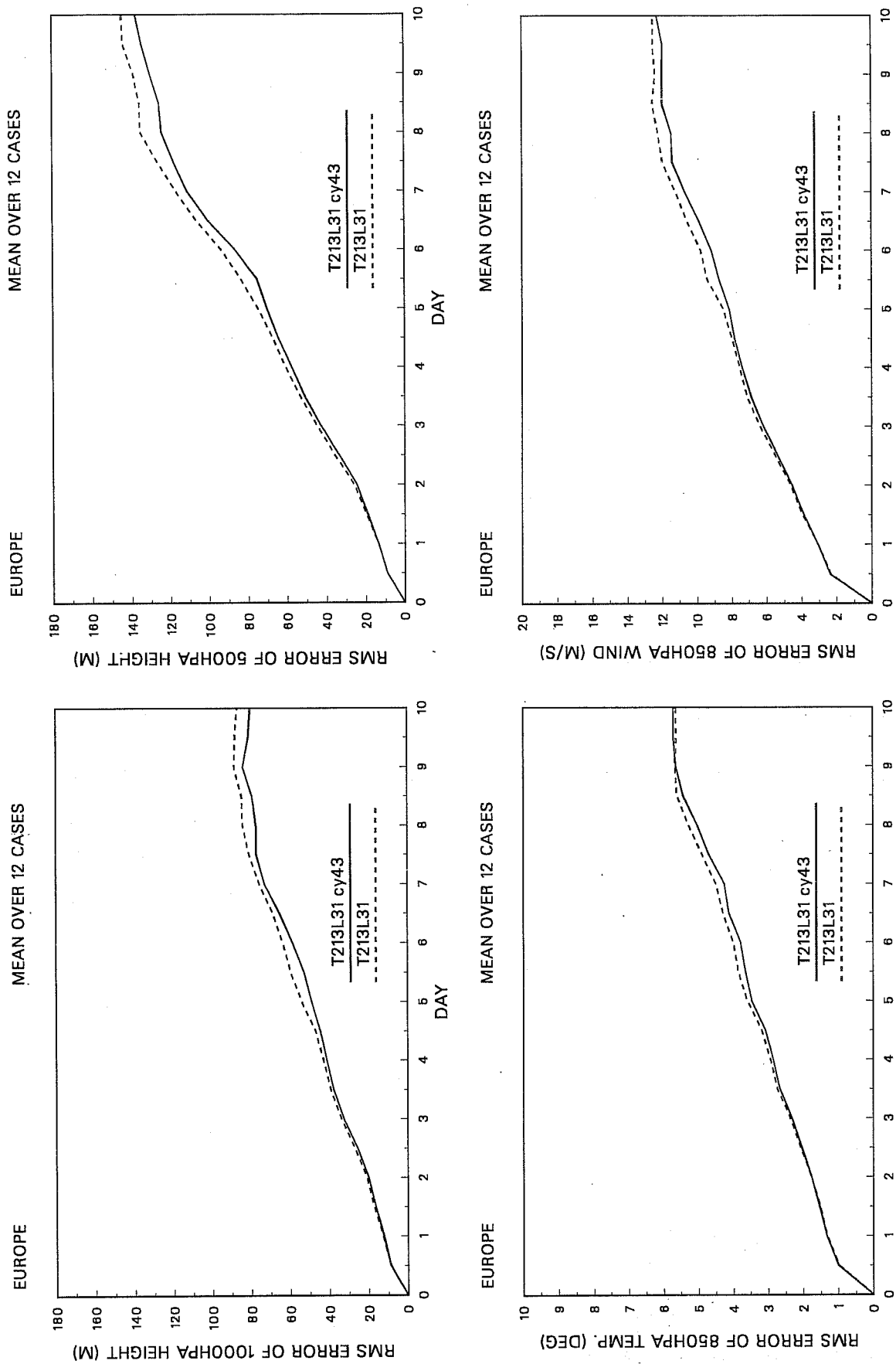

Fig. 11 RMS errors of 1000 and 500hPa height and of 850hPa temperature and vector wind, using the initial version of model cycle 43 (solid lines) and model cycle 42 (dashed lines), averaged over twelve T213/L31 forecasts.

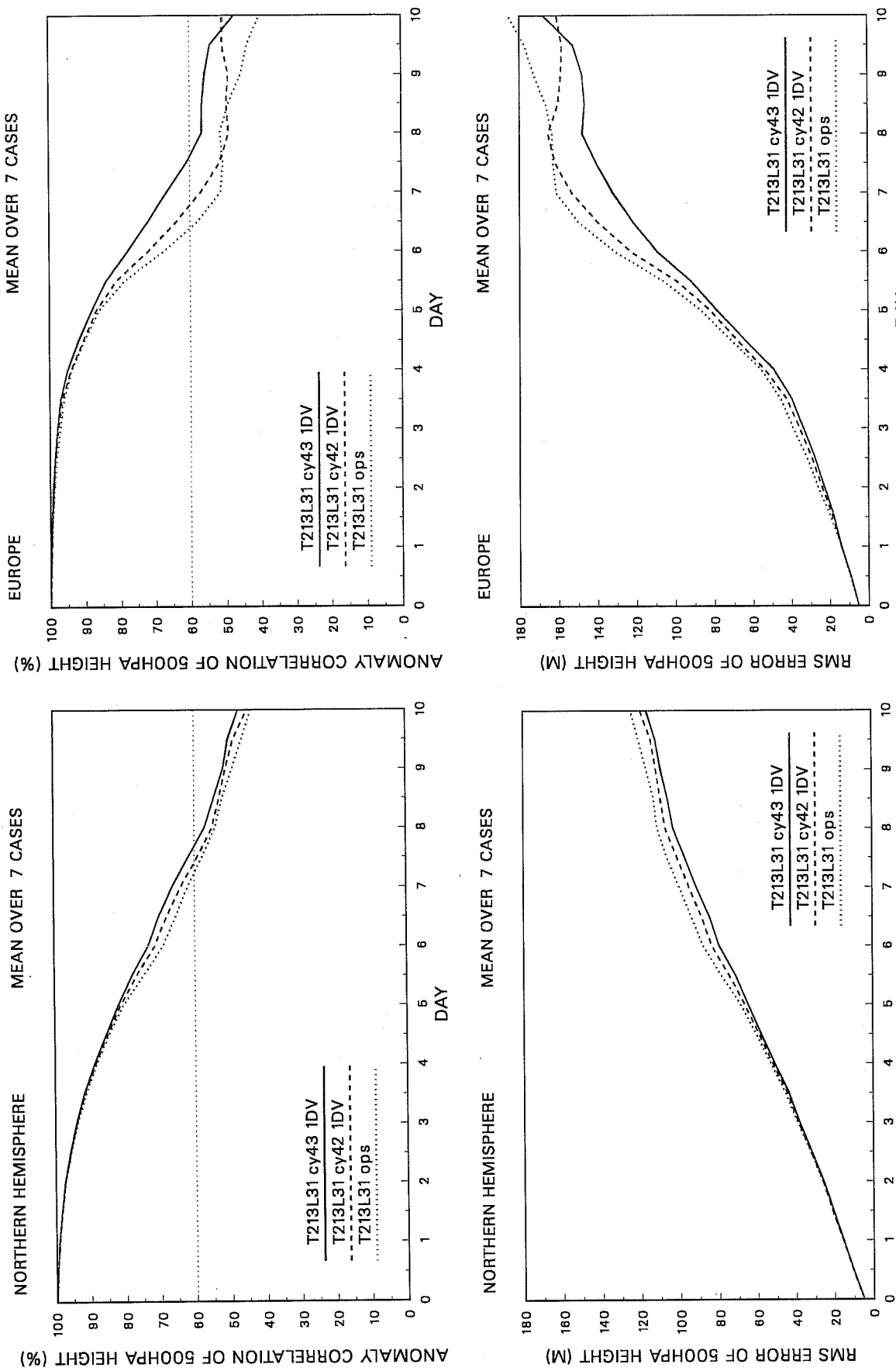

Fig. 12 500hPa height anomaly correlations and RMS errors for the extratropical Northern and Hemisphere and Europe, for T213/L31 forecasts using the initial version of model cycle 43 (solid lines), and model cycle 42 (dashed lines), with data assimilation using the operational analysis system as of 1 July 1992, and for operations (dotted lines). Averages for the period 13 to 19 January 1992 are shown.

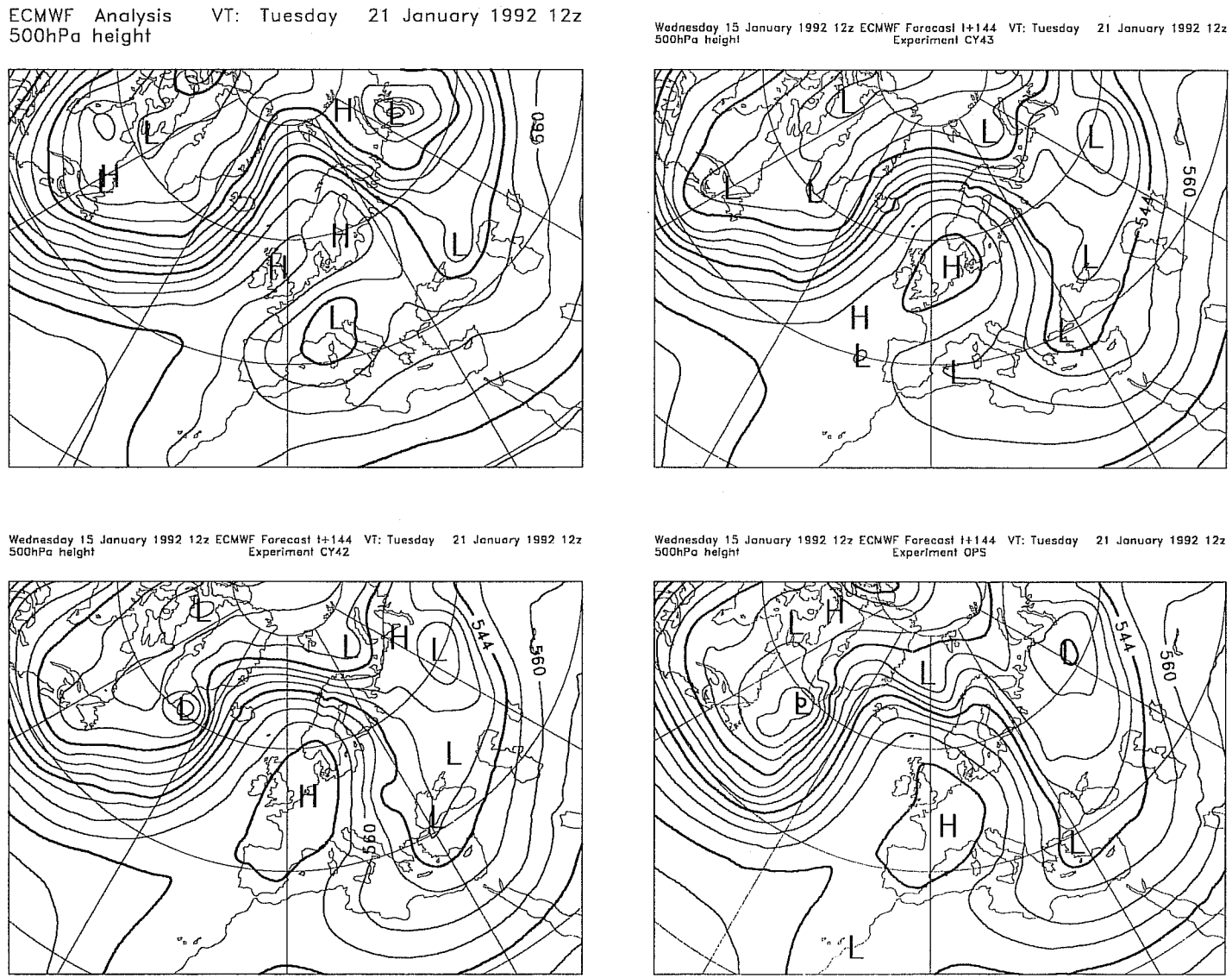

Fig. 13 Operational 500hPa height analyses (contour interval 8dam, upper left) and verifying day-6 forecasts from reassimilations with the provisional cycle 43 (upper right) and cycle 42 (lower left). The corresponding operational forecasts are shown lower right. Verifying dates are: a) 21 January 1992

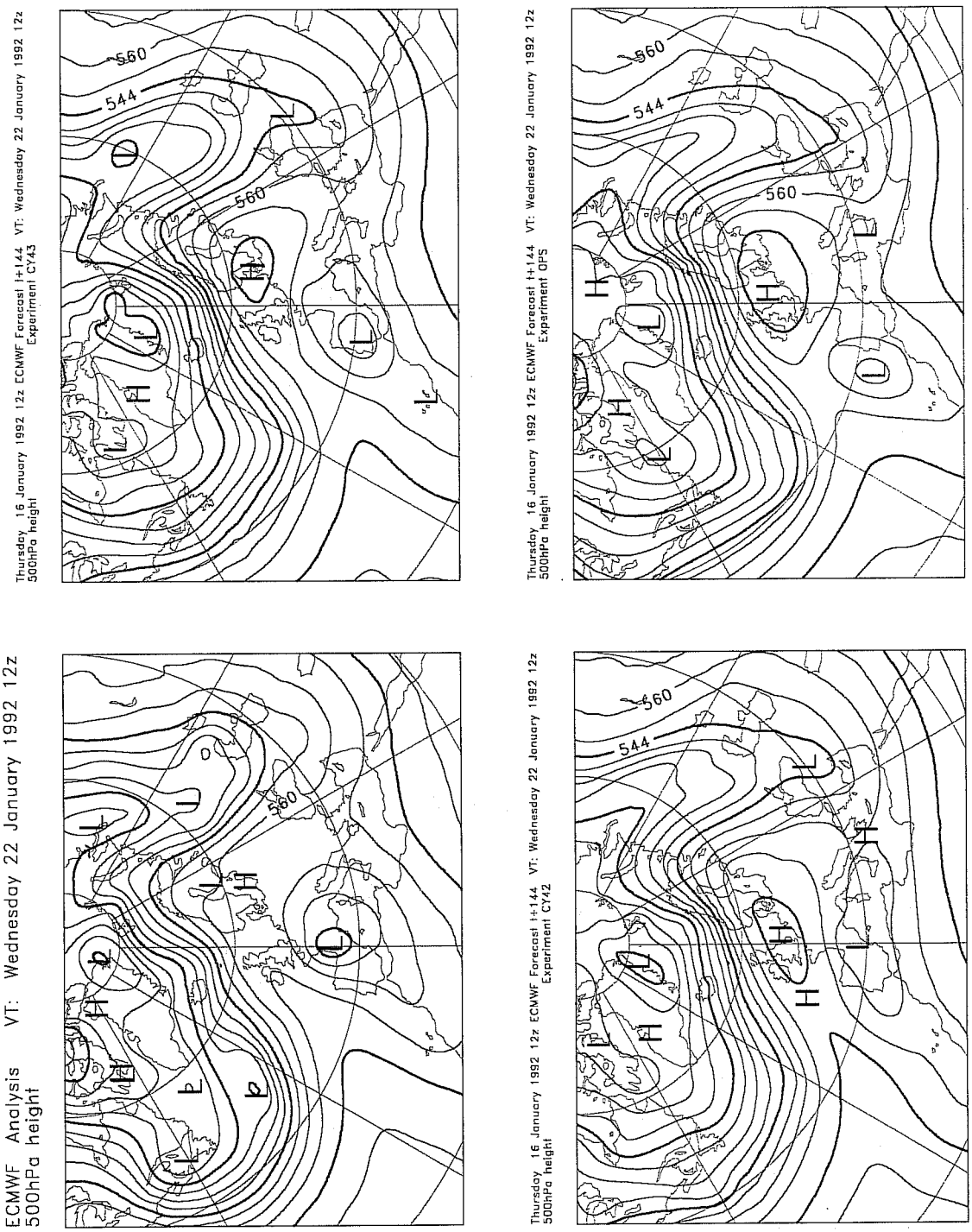

Fig. 13 b) 22 January 1992

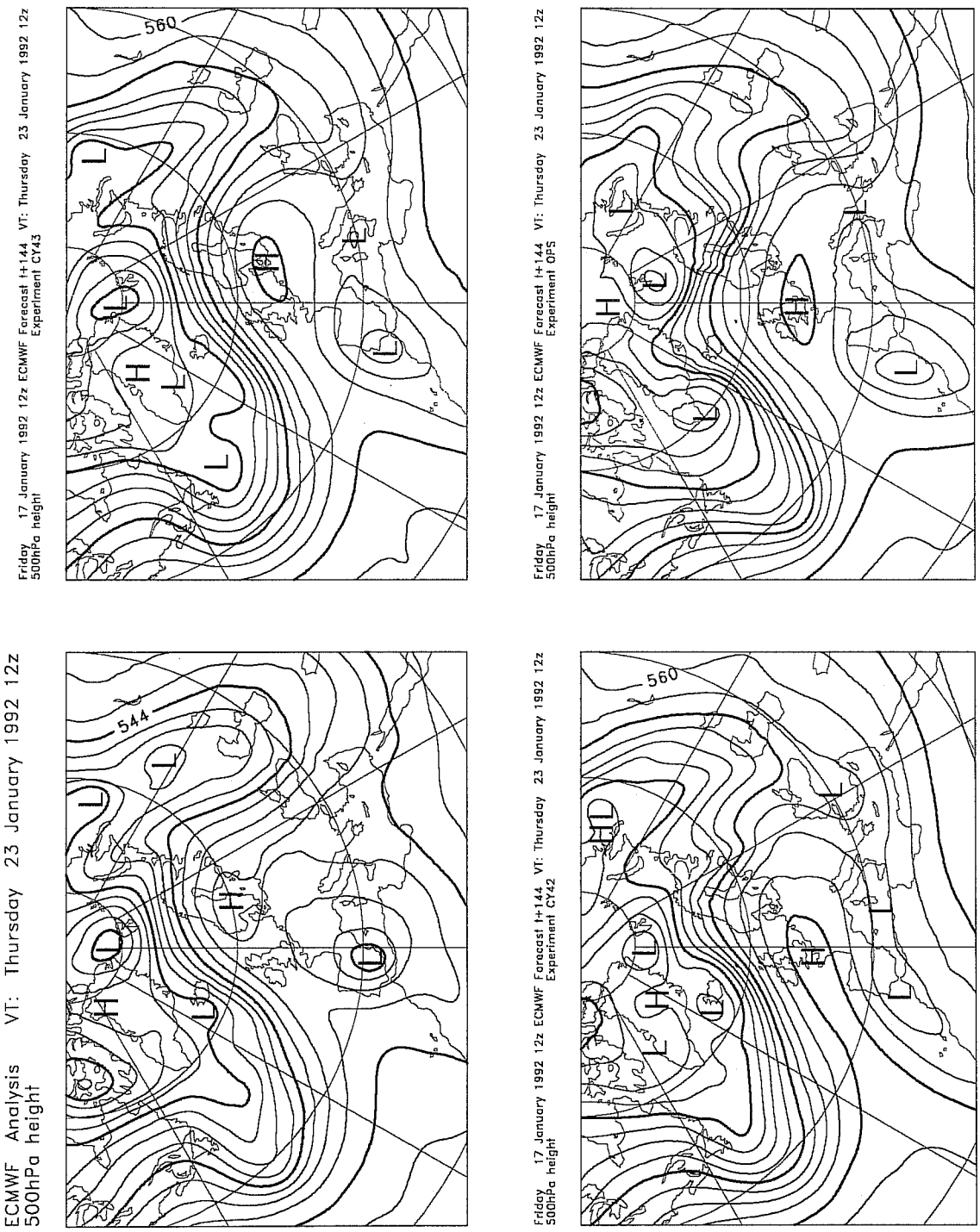

Fig. 13 c) 23 January 1992

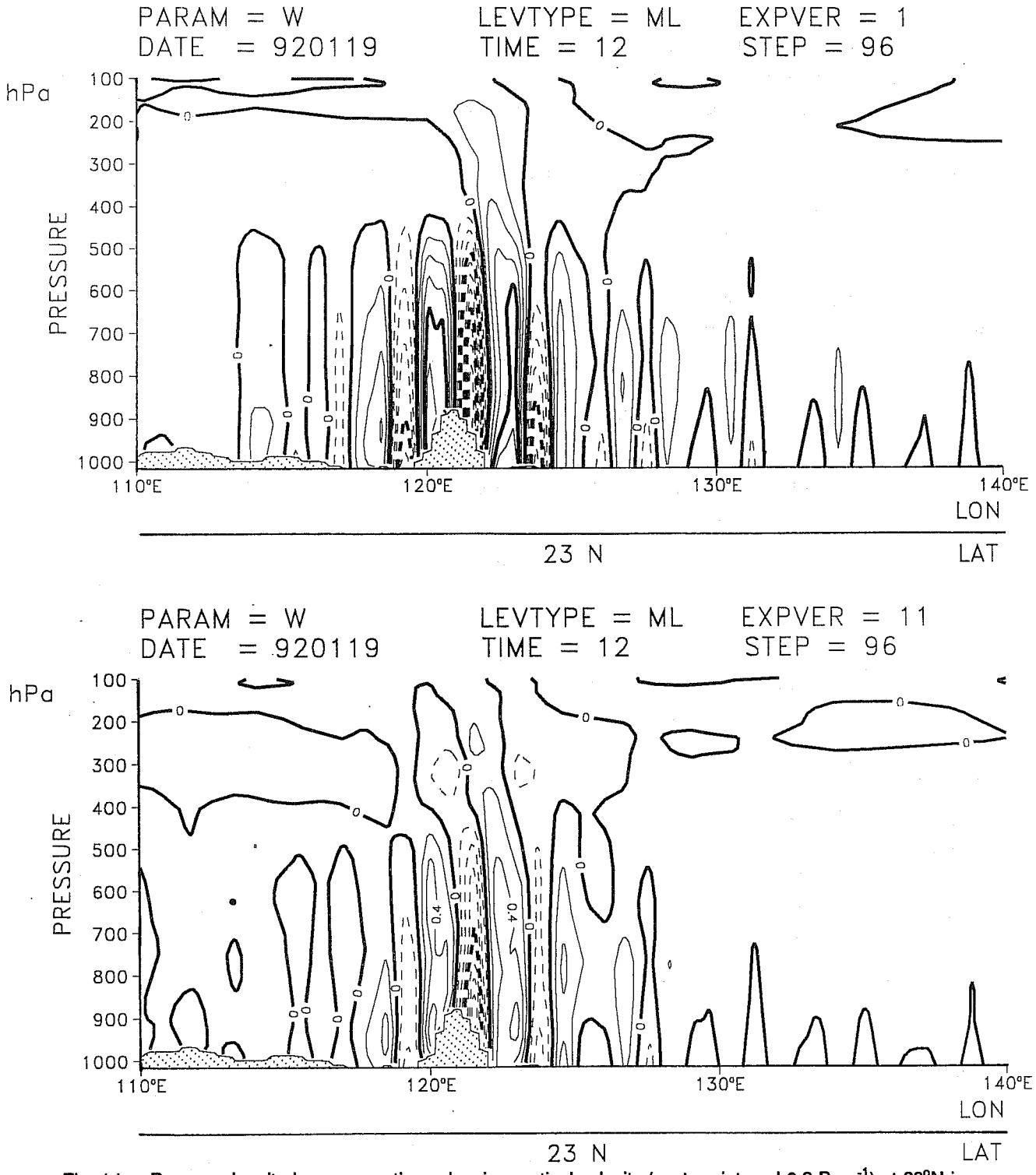

Fig. 14 Pressure-longitude cross-sections showing vertical velocity (contour interval 0.2 Pa s^{-1}) at 23°N in the vicinity of Taiwan. The upper plot displays the operational day-4 forecast from 19 January 1992, and the lower plot shows the corresponding forecast using the provisional cycle 43.

of reduced horizontal diffusion, the reduction in time step from 20 to 15 minutes plays a beneficial role in this respect.

The lower damping is also seen clearly in stratospheric potential vorticity maps such as discussed by Pyle at this Seminar. The upper plot of Fig. 15 presents the isentropic PV for the 475K surface from the day-5 forecast starting 19 January 1992 using cycle 43. It shows a pronounced intrusion of low-PV air into the polar region. Shortly after the time shown, this air becomes cut off within the polar vortex as the latter re-establishes its more normal weakly distorted circumpolar form. The lower plot of Fig. 15 shows the corresponding operational forecast, which exhibits generally weaker PV gradients, and a less sharp picture of the intrusion of low-PV air. Weaker extrusion of higher PV air away from the vortex can also be seen in the Pacific/North American sector.

It was expected that the new version of the model would reduce the day-to-day inconsistency of forecasts, given its lower (and more realistic) level of eddy activity. This has been confirmed in general. Fig. 16 shows RMS differences between consecutive forecasts as functions of forecast range averaged over the six pairs of forecasts from the January assimilation experiment. Results are shown for 500 hPa height for the extratropical hemispheres and for Europe, and for 850 hPa wind for the tropical belt. The general reduction of differences due to use of the new model version is clear. Moreover, the increase in inconsistency beyond day 7.5 seen for the Northern Hemisphere largely disappears when the Arctic is removed from the domain. The removal of fixed, climatological sea-ice temperatures is presumably responsible for an increase in variability at very high latitudes in winter.

During the course of this experiment it was realised that a pronounced radiative cooling in the subtropics close to the model level $\eta = 0.8$ was caused by an artificial limitation of the height of the inversion cloud. The new model version was accordingly modified, and a summer data assimilation was run. Because of a strong sensitivity of 850 hPa temperature forecasts in part of the Northern Hemisphere, and of height forecasts for the Southern Hemisphere, the experiment was continued for two weeks, from 24 June to 7 July. 500 hPa height scores, presented in Fig. 17, again show beneficial impact of the model change over the Northern Hemisphere as a whole, and Europe in particular, although not to the extent seen in the January experiment. 850 hPa temperature scores for the Northern Hemisphere were generally poorer with cycle 43. This was not seen over Europe and the North Atlantic, differences being largest over the Arctic and North Pacific, and downstream over North America. Height forecasts for the Southern Hemisphere showed a highly variable impact of the model change from case to case, but little sensitivity in the mean. For all parameters, day-to-day consistency was either similar or better with cycle 43, as measured by RMS differences between consecutive forecasts (Fig.18). Moreover, a set of five forecasts with cycle 43 from operational (cycle 42) analyses for dates earlier in June 1992 showed no such deterioration in 850 hPa temperature forecasts, and improved height forecasts for the Southern Hemisphere.

The above results were judged to be sufficient to justify the operational implementation of the new model version in mid-August. A correction to the non-interpolating semi-Lagrangian scheme had to be made at the beginning of September with the introduction of model cycle 44; this resulted in a slight further improvement in forecast skill scores.

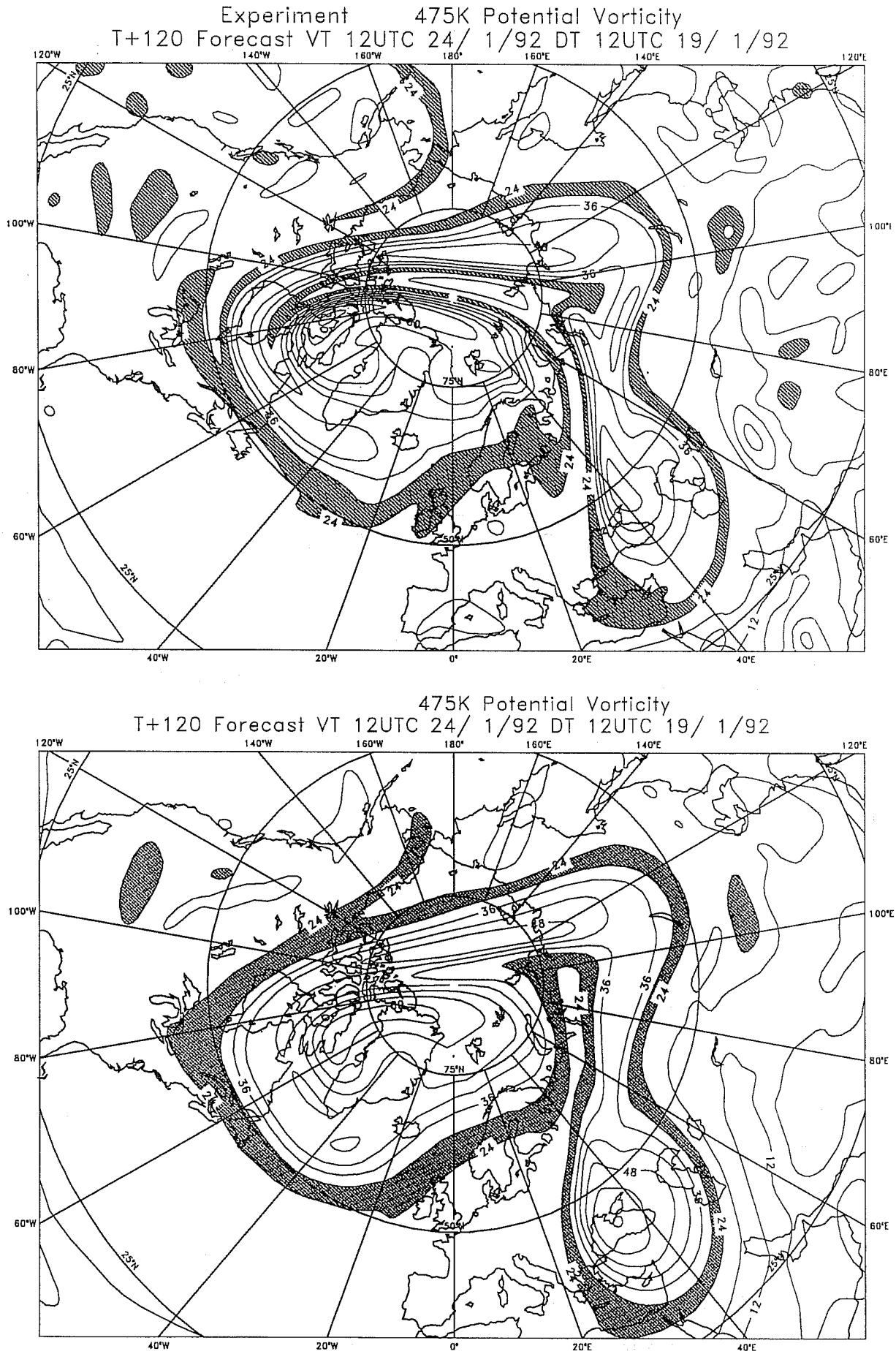

Fig. 15 Potential vorticity on the 475K isentropic surface for day-5 forecasts from 19 January 1992. The upper plot shows the forecast using the provisional cycle 43 version of the model, the lower plot shows the corresponding operational forecast.

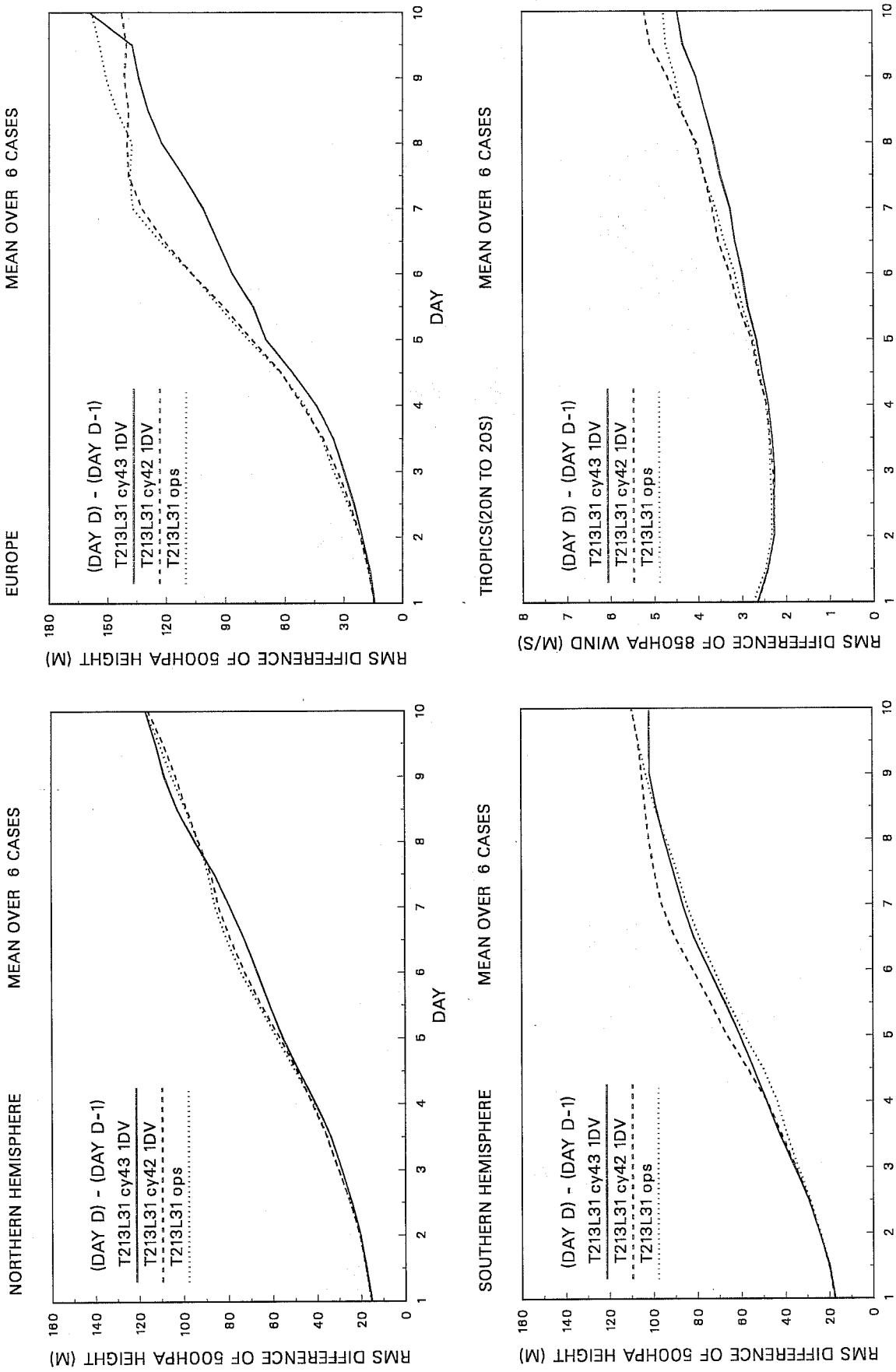

Fig. 16 RMS differences between consecutive forecasts of 500hPa height for the Northern and Southern Hemispheres, and for Europe, and of 850hPa vector wind for the Tropics. The cases are as in Fig. 32.

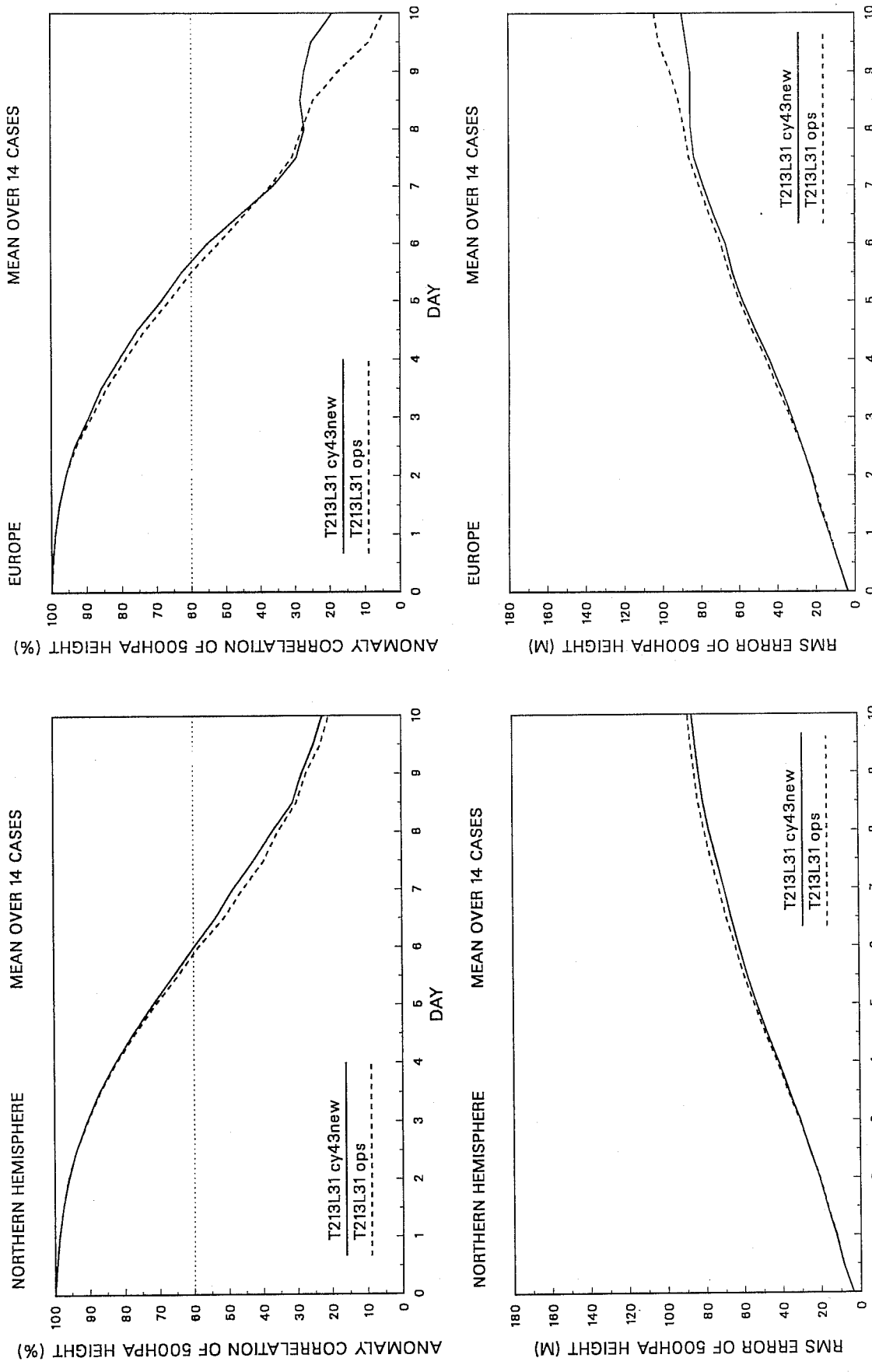

Fig. 17 500hPa height anomaly correlations and RMS errors for the extratropical Northern Hemisphere and Europe, for T213/L31 forecasts using model cycle 43 (solid lines) and the operational model cycle 42 (dashed lines). Averages are for the period 24 June to 7 July 1992.

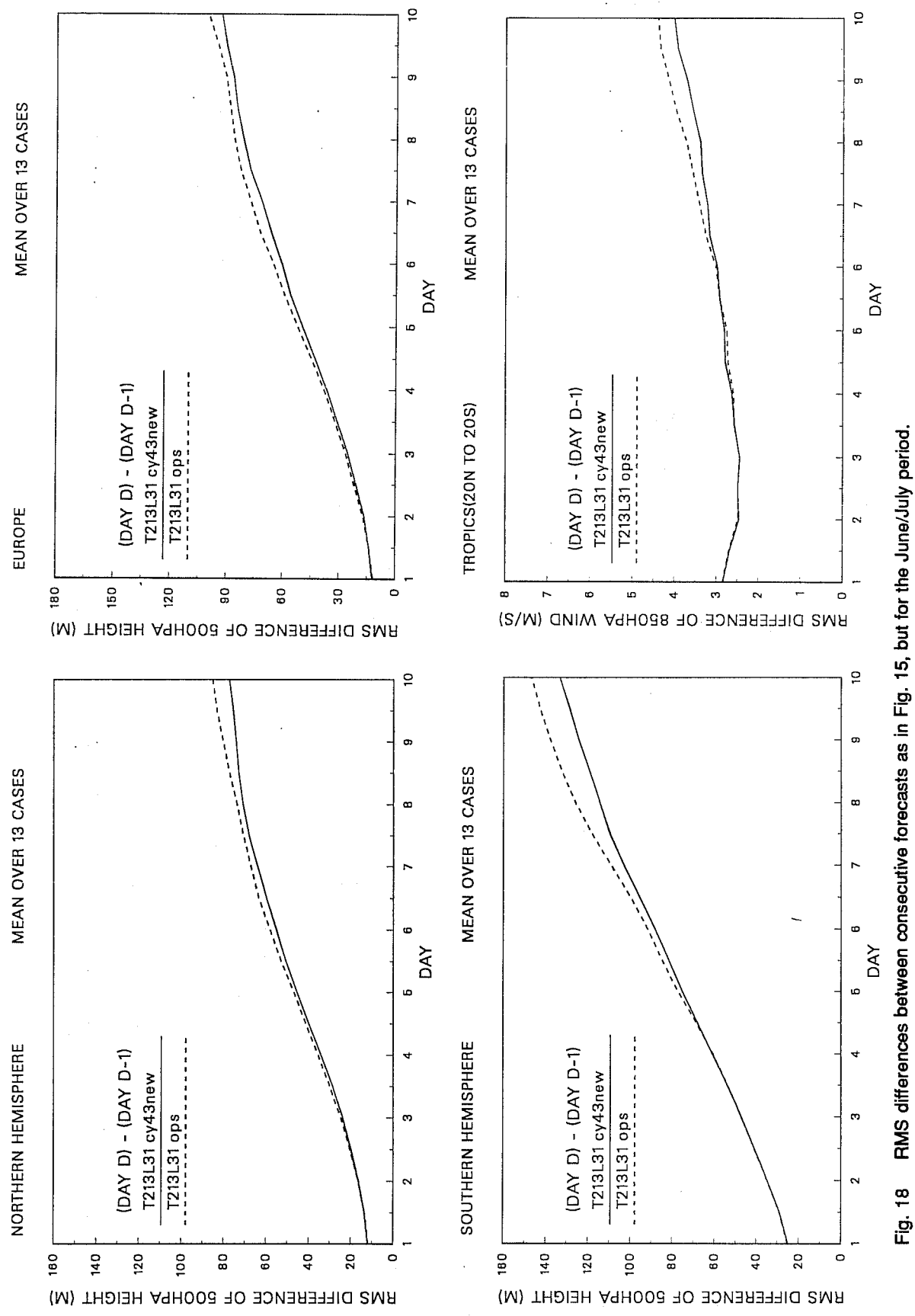

Fig. 18 RMS differences between consecutive forecasts as in Fig. 15, but for the June/July period.

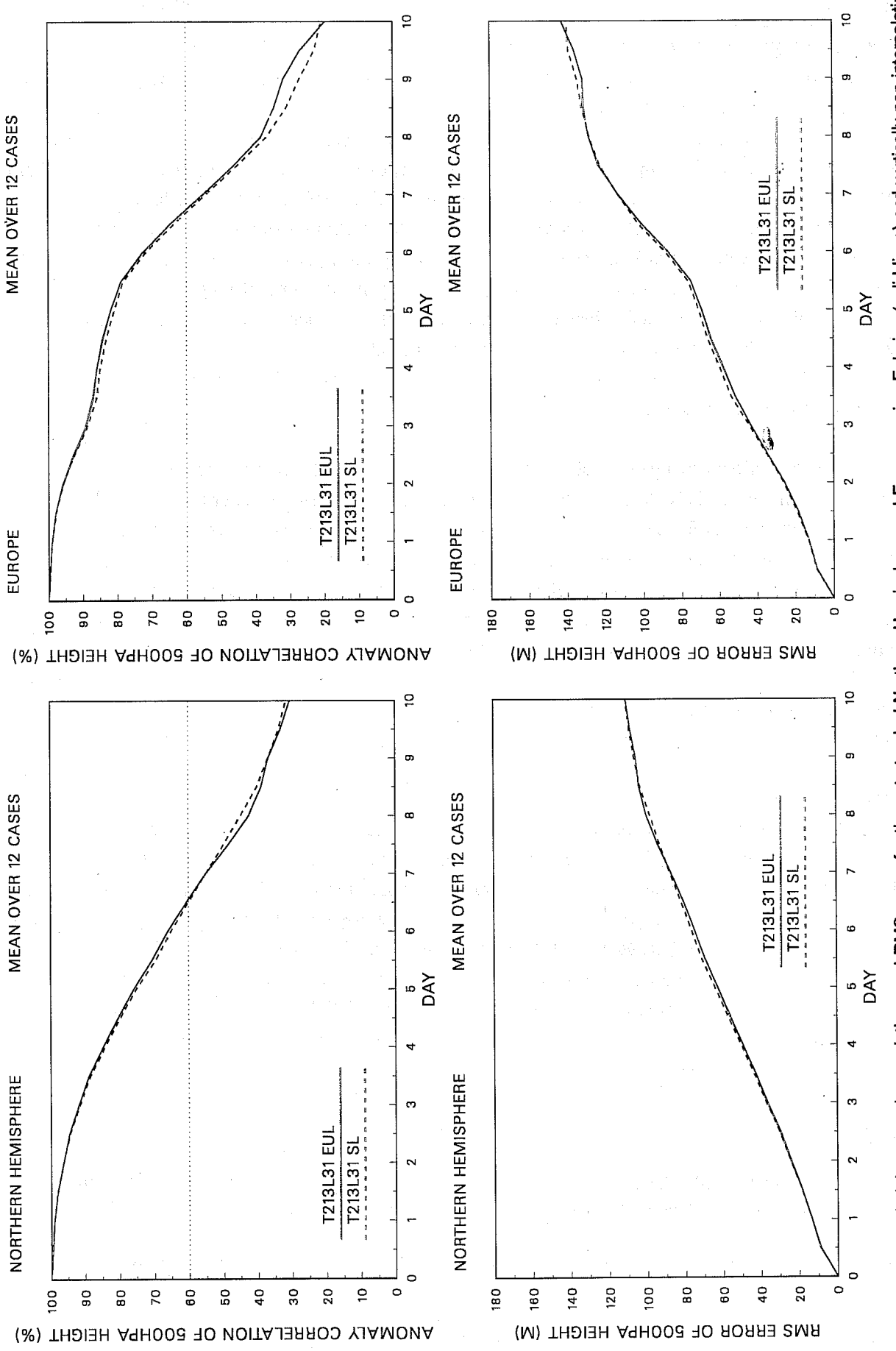

Fig. 19 500hPa height anomaly correlations and RMS errors for the extratropical Northern Hemisphere and Europe, using Eulerian (solid lines) and vertically non-interpolating semi-Lagrangian (dashed lines) advection schemes, averaged over twelve T213L31 forecasts.

6. ONGOING WORK

The model changes introduced operationally this summer address some deficiencies of the T213/L31 model, but do not provide complete answers. In particular, radiative cooling of the upper troposphere appears to be too large, and this is thought to be an additional source of the model's excessive eddy activity. This problem is worse with 31 than with 19 levels. Several possible changes to the cloud/radiation parametrization are under investigation, most notably in the specification of cloud optical properties. Some promising results have been obtained, but further work is required before operational implementation can be considered. These changes will also have an impact on the solar radiation received at the surface, and this together with continuing work on the surface and boundary-layer parametrization should lead to further reduction of systematic errors in two-metre temperatures. A principal area of longer term research is the development of a prognostic cloud scheme to replace the current diagnostic approach. In view of this, we do not plan significant further development of the diagnostic scheme, for example to seek a solution to the low cloud problems that is better than the rather arbitrary suppression of the "inversion-cloud" component in the lowest three model layers.

Soon after the operational change to cycle 43, the new CRAY Y-MP C90 computer became available to run numerical experiments at ECMWF. This enabled a substantial comparison of Eulerian and semi-Lagrangian forecasts to be carried out for the first time at T213/L31 resolution. This comparison showed that the non-interpolating scheme introduced with cycle 43 resolved much of the difference in performance between semi-Lagrangian and Eulerian versions of the high-resolution model. Fig. 19 presents some 500 hPa height verifications for a set of twelve Eulerian and vertically non-interpolating semi-Lagrangian forecasts. Differences in skill score are evidently small, but they nevertheless still favour the Eulerian version of the model. Moreover, levels of eddy kinetic energy are still somewhat higher in the set of semi-Lagrangian forecasts, and comparisons of skill scores for lower horizontal and vertical resolutions show larger differences in favour of the Eulerian scheme. Study of the semi-Lagrangian formulation is thus continuing.

Acknowledgements

Many colleagues participated in the studies presented here. The original formulation and coding of the semi-Lagrangian scheme carried out by Hal Ritchie during a visit to ECMWF included the option of the vertically non-interpolating version. Clive Temperton, Mariano Hortal and Terry Davies worked together with the author on numerical aspects of the work, and all members of the parametrization section were involved to some extent or other: Martin Miller (clouds and general validation), Pedro Viterbo (sea-ice and general validation), Jean-Jacques Morcrette (radiation and clouds), Anton Beljaars (boundary layer), Lodovica Illari (spin-up) and Michael Tiedtke (convection). Ernst Klinker contributed significantly through his routine monthly diagnostic studies and diagnosis of the tests of cycle 43, and Cedo Brankovic carried out the extended-range integrations.

References

Eyre, J.R., G.A. Kelly, A.P. McNally and E. Andersson, 1992: Assimilation of TOVS radiance information through one-dimensional variational analysis. ECMWF Technical Memorandum No. 187, 31 pp.

Hortal, M., 1991: Formulation of the ECMWF model. Proceedings of 1991 ECMWF Seminar on Numerical Methods in Atmospheric Models, II, 261-280.

Ritchie, H., 1991: Application of the semi-Lagrangian method to a multilevel spectral primitive-equation model. Quart.J.Roy.Met.Soc., 117, 91-106.

Simmons, A.J., 1991: Development of a high resolution, semi-Lagrangian version of the ECMWF forecast model. Proceedings of 1991 ECMWF Seminar on Numerical Methods in Atmospheric Models, II, 281-324.